Crosstalk Between Nuclear MET and SOX9/β-Catenin Correlates with Castration-Resistant Prostate Cancer

Yingqiu Xie, Wenfu Lu, Shenji Liu, Qing Yang, Brett S. Carver, Estelle Li, Yuzhuo Wang, Ladan Fazli, Martin Gleave, and Zhenbang Chen

Department of Biochemistry and Cancer Biology (Y.X., W.L., S.L., Q.Y., Z.C.), Meharry Medical College, Nashville, Tennessee 37208; Department of Surgery and Division of Urology (B.S.C.), Memorial Sloan-Kettering Cancer Center, New York, New York 10065; and Vancouver Prostate Centre and Department of Urologic Sciences (E.L., Y.W., L.F., M.G.), The University of British Columbia, Vancouver, British Columbia, Canada V6H 3Z6

Castration-resistant prostate cancer (PCa) (CRPC) is relapse after various forms of androgen ablation therapy and causes a major mortality in PCa patients, yet the mechanism remains poorly understood. Here, we report the nuclear form of mesenchymal epithelial transition factor (nMET) is essential for CRPC. Specifically, nMET is remarkably increased in human CRPC samples compared with naïve samples. Androgen deprivation induces endogenous nMET and promotes cell proliferation and stem-like cell self-renewal in androgen-nonresponsive PCa cells. Mechanistically, nMET activates SRY (sex determining region Y)-box9, β-catenin, and Nanog homeobox and promotes sphere formation in the absence of androgen stimulus. Combined treatment of MET and β-catenin enhances the inhibition of PCa cell growth. Importantly, MET accumulation is detected in nucleus of recurrent prostate tumors of castrated *Pten/Trp53* null mice, whereas MET elevation is predominantly found in membrane of naïve tumors. Our findings reveal for the first time an essential role of nMET association with SOX9/β-catenin in CRPC in vitro and in vivo, highlighting that nuclear RTK activate cell reprogramming to drive recurrence, and targeting nMET would be a new avenue to treat recurrent cancers. **(*Molecular Endocrinology* 28: 1629–1639, 2014)**

Prostate cancer (PCa) is the second leading cause of cancer-related deaths among American men. Androgen deprivation therapy is commonly used to treat advanced PCa, but the development of castration-resistant PCa (CRPC) resulted in the failure to androgen deprivation therapy (1). Nonhormone therapy, such as docetaxel-related chemotherapy, is also employed to treat CRPC (2), yet multiple drug resistance often occurs or arises through Notch/hedgehog signaling (3) or reprogramming factors-mediated tumor initiation (4). The progressive malignancy of CRPC is contributed by aberrant activations of oncogenic signaling pathways, including AKT (5, 6), Pim-1 proto-oncogene (7), and Rous sarcoma virus (8), through the altered expression (9) or activity (10) of androgen receptor (AR). MET (mesenchymal epithelial transition factor) is a membrane-bound receptor tyrosine kinase (RTK) activated by hepatocyte growth factor (HGF) to promote tumor growth and metastasis in various cancers, including PCa (11). Upon HGF binding, the membrane bound or membraneous form of MET (mMET) (or c-MET, also called MET) with the autophosphorylation at Y1234/1235 provides a docking site for growth factor receptor bound protein binding followed by the activation of downstream signaling, such as AKT and MAPK (11). AR inhibits *MET* transcription in prostates (12), suggesting that AR antagonist in turn may

ISSN Print 0888-8809 ISSN Online 1944-9917
Printed in U.S.A.

Received March 7, 2014. Accepted July 30, 2014.
First Published Online August 6, 2014

Abbreviations: AR, androgen receptor; cFBS, charcoal-stripped FBS; CRPC, castration-resistant PCa; EGFR, epidermal growth factor receptor; FBS, fetal bovine serum; GFP, green fluorescent protein; H&E, hematoxylin and eosin; HGF, hepatocyte growth factor; IB, immunoblotting; IF, immunofluorescence; IHC, immunohistochemistry; MET, mesenchymal epithelial transition factor; mMET, membraneous form of MET; nMET, nuclear form of MET; NANOG, Nanog homebox; OCT4, octamer-binding transcription factor 4; PCa, prostate cancer; PI3K, phosphatidylinositol 3-kinase; PTEN, phosphatase and tensin homolog deleted on chromosome 10; RTK, receptor tyrosine kinase; SOX9, SRY (sex determining region Y)-box9; TMA, tissue microarray; Wnt, Wingless-related integration site.

result in the up-regulation of MET in CRPC. MET inhibition by crizotinib, approved for the treatment of nonsmall cell lung cancer in the United States, reduced PCa growth in mice (13). However, drugs targeting elevations of mMET (or c-MET) often are revoked by resistance in cancers (14). Recently, MET was detected in nucleus of breast cancer (15) and hepatocellular carcinoma cells (16). Interestingly, nuclear form of MET (nMET) showed an activity of ectodomain shedding kinase in breast cancer cells in a ligand-independent manner (17, 18). The molecular mechanisms and downstream signaling of aberrant nMET remain elusive, and its relevance to malignancy recurrence is not known.

SOX9, a transcription factor of SOX (SRY [sex determining region Y]-related high mobility group box) family, is required to activate autoregulatory programs to induce and maintain the stem cell state in mammary glands (19), the progenitor cell pool in pancreas (20), as well as cancer development in prostates (21). Moreover, SOX9 expression requires β-catenin to generate the impact in PCa growth (22), whereas Wingless-related integration site (Wnt)/β-catenin activation shows its essential role in CRPC by targeting downstream targets, including AR (23). Most recently, the role of Wnt/β-catenin was reported to associate with the reprogramming of retinal neurons (24). Strikingly, SOX9 or β-catenin (25) cooperates with phosphatase and tensin homolog deleted on chromosome 10 (Pten) inactivation to accelerate PCa progression, which may contribute to CRPC growth of prostate tumors in mice (26). On another hand, the resistance traits of CRPC growth caused by Pten inactivation with an additional deletion of either *Trp53* or *Zbtb7a* can be significantly suppressed by the combined inhibition of X-linked inhibitor of apoptosis protein, steroid 5-alpha-reductase type I, and AR signaling pathways in vivo (27). Therefore, besides PTEN/phosphatidylinositol 3-kinase (PI3K)/AKT pathway, combined targeting of additional pathways, such as SOX9 or β-catenin, may be an effective strategy to control PTEN loss-induced CRPC progression. Here, we demonstrated a novel oncogenic role of nuclear MET in CRPC in vitro using androgen-nonresponsive cell culture systems and in vivo using a unique *Pten/Trp53* mouse model and human CRPC specimens.

Materials and Methods

Additional details are described in Supplemental Figures 1–6.

Cell culture and establishment of stable cell line

C4–2B (M.D. Anderson, Houston, Texas), PC3 (American Type Culture Collection), and human PCa cells were maintained in RPMI 1640 supplemented with 10% fetal bovine serum (FBS) (Life Technologies) and 1% penicillin/streptomycin (Life Technologies) at 37°C with 5% CO_2. LAPC4 (a gift from Dr Charles L. Sawyers) and 22Rv1 and 293FT (American Type Culture Collection) cells were grown in DMEM supplemented with 10% FBS and 1% penicillin/streptomycin at 37°C with 5% CO_2. PCa cell lines with MET overexpression were established by lentiviral infection and selection. Briefly, 293FT cells were cotransfected using Lipofectamine 2000 (Life Technologies) with lentivirus packaging plasmid and MET plasmid (Addgene plasmid 37560, 37561) or Vector-green fluorescent protein (GFP) (Addgene 17448). Forty-eight hours after transfection, viral supernatants were collected for viral infection, and infected PCa cells were selected by puromycin (2 μg/mL) for 2 days.

Immunoblotting (IB), protein ubiquitination assay, and immunofluorescence (IF)

For IB, cell lysates were harvested in buffer (20mM Tris-HCl [pH 7.4], 150mM NaCl, 1mM EDTA, 1mM EGTA, and 1% Triton X-100) with protease inhibitor cocktail (Roche) followed by standard procedures of SDS-PAGE and antibody detection. To study protein ubiquitination, cells in serum starvation for 48 hours were treated with MG-132 (an inhibitor of proteasome) (Sigma-Aldrich) at 15μM for 4 hours, and cell lysates were collected using denatured buffer (8M urea and 0.1M Na_2HPO_4/NaH_2PO_4) followed by 1:20 dilution, immunoprecipitation and IB for ubiquitination assay as described previously (28, 29). For IF analysis, cells grown on coverslips for 2 days were fixed in 4% paraformaldehyde or ice-cold methanol for 15 minutes. Cells on slides were probed using primary antibodies: MET (C28, sc-161, 1:100; Santa Cruz Biotechnology, Inc), MET (D1C2, 1:50; Cell Signaling), MET (3D4, 1:100; Life Technologies), SOX9 (H90, sc-20095, 1:00; Santa Cruz Biotechnology, Inc), Nanog homebox (NANOG) (D73G4, 4903, 1:50; Cell Signaling), octamer-binding transcription factor 4 (OCT4) (C30A3, 2840, 1:50; Cell Signaling), or β-catenin (6B3, 9582, 1:100; Cell Signaling) overnight at 4°C, followed by incubation with secondary antibodies Alexa Fluor 568 (A10042 and A10037, 1:200; Life Technologies) or Alexa Fluor 488 (A11070 and A11017, 1:200; Life Technologies). Slides were washed with PBS, stained with 4′,6-diamidino-2-phenylindole (DAPI) and mounted with Vectashield (Vector Laboratories), and images were scanned with laser confocal microscopy (Nikon A1R).

Mutant mice, tumor analysis, and immunohistochemistry (IHC)

Mice were bred and maintained in accordance with the guidelines of the protocol approved by the Institutional Animal Care and Use Committee of Meharry Medical College. *Pten*$^{lox/lox}$, *Trp53*$^{lox/lox}$, and *PB-Cre4* mice were maintained as described previously (30). All experimental animals were kept in a mixed genetic background of C57BL/6J X129/DBA2. All genotypes were verified by PCR with primers and conditions as described previously. Mice of desired genotypes were randomly divided into 2 groups with or without castration at 3 months of age. Mice were euthanized at 6 months of age, and anterior prostates or prostate tumors were dissected and collected. Tissues were fixed and processed according to standard protocols, and tissue sections in 5-μm thickness were used for hematoxylin and eosin (H&E) and IHC staining. For IHC analysis, sections were stained using primary antibodies to MET (C28, sc-161, 1:500;

Santa Cruz Biotechnology, Inc), SOX9 (H90, sc-20095, 1:00; Santa Cruz Biotechnology, Inc), β-catenin (6B3, 9582, 1:100; Cell Signaling), or Ki67 (SP6, ab16667, 1:200; Abcam).

Human prostate tissue microarrays (TMAs)

For CRPC TMA, human prostate TMAs slides containing paraffin-embedded 28 CRPC tumors and 25 primary tumor control samples were obtained from Vancouver Prostate Centre Tissue Bank (http://www.prostatecentre.com). H&E slides were reviewed, the desired areas were marked, and their correspondent paraffin blocks were used for manually TMA construction (Beecher Instruments) by punching duplicate or triplicate cores of 1 mm for each sample. All specimens were from radical prostatectomy with consents from patients at Vancouver Prostate Centre (http://www.prostatecentre.com). Tissue sections were stained using primary antibodies MET (3D4, 1:50; Life Technologies) and MET (EP1454Y, 1:50; Abcam). The staining intensity and extent were evaluated blindly and graded on a scale of 0 (negative) to 3 (strong positive). Scores were compared with different stages of cancer.

Results

Nuclear MET is accumulated in malignant cells of human CRPC specimens

In order to understand the oncogenic contribution of MET to CRPC growth, we applied CRPC TMA of human PCa samples to compare the levels of mMET (or c-MET) between naïve PCa and CRPC specimens. As expected, mMET levels, confirmed by MET (EP1454Y) antibody that is raised against the N terminus (transmembrane domain) of MET, are elevated in both naïve PCa and CRPC specimens. However, mMET were strikingly elevated for most malignant cells in CRPC samples as compared with some lesions in naïve PCa specimens (Supplemental Figure 1). Paradoxically, the positivity for mMET (89%, 25/28) in CRPC specimens was comparable with that (100%, 25/25) in naïve PCa specimens ($P = .42$) (Figure 1, A and B), indicating that mMET may not directly contribute to CRPC growth. We then went to investigate whether nMET accumulation was differentially elevated between CRPC groups and naïve PCa groups of those human PCa specimens. Because nMET is the nMET cleaved the N-terminal transmembrane domain (15), we chose to use the MET antibody (3D4) raised against the C-terminal fragment of MET, which contains the cytoplasmic but not the transmembrane domain, to compare the nMET expression levels between CRPC and naïve PCa samples. Surprisingly, cases positive for nMET were much higher in CRPC (75%, 21/28) than that in naïve PCa samples (44%, 11/25) (Figure 1A). nMET expression level in CRPC specimens was significantly increased than that in naïve PCa ($P < .01$) (Figure 1B), and the localization of nMET was restrained to the nucleus of malignant cells (Figure 1C). nMET positivity occurs significantly delayed than mMET positivity in CRPC cases (Figure 1D), supporting the notion that nMET is likely derived from mMET with an important role in recurrence.

A

	mMET			nMET		
Positivity	+	-	%	+	-	%
Naïve	25	0	100	11	14	44
CRPC	25	3	89	21	7	75

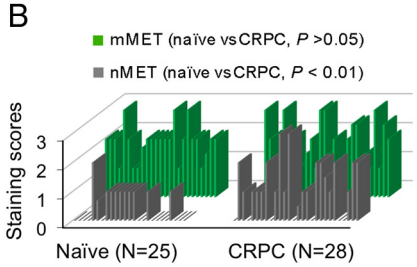

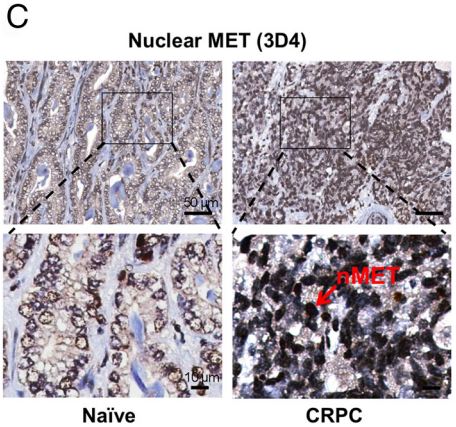

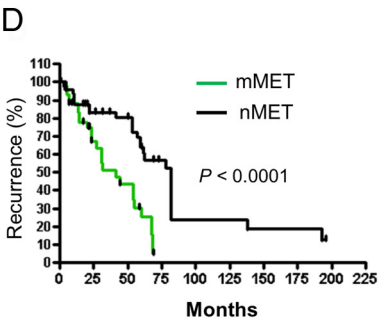

Figure 1. Nuclear MET is elevated in human CRPC specimens. A, The positivity of MET (mMET and nMET) among individual PCa specimens. B, The scores of MET staining among individual PCa specimens. Scores are presented as the average for individual patient samples in duplicate or triplicate. $P > .05$, mMET for CRPC vs naïve PCa; $P < .01$, nMET for CRPC vs naïve PCa. C, IHC images to show the localizations of nuclear MET in naïve and CRPC specimens. Scale bars, 100 μm. Patient samples were stained in duplicate or triplicate. D, Kaplan-Meijer plot to show the recurrence percentage of mMET and nMET in CRPC samples; n = 97 samples, $P < .0001$.

Androgen deprivation induces the elevation of endogenous nuclear MET

We wished to understand the regulation and biological function of nMET in PCa cells and then examined the expression of total MET in both androgen-nonresponsive (DU145, PC3, C4–2B, and 22Rv1) and androgen-responsive (LAPC4 and LNCaP) cell lines. IB results showed that MET level is strikingly elevated in DU145 and PC3 cell lines that are AR negative, as compared with other cell lines (Supplemental Figure 2A). Activations of tyrosine

kinases and their abnormal accumulations in cellular compartments are the consequent oncogenic events frequently observed in various cancers (31). Given the remarkable elevations of MET in PCa specimens, we asked ourselves whether the elevation and the nuclear accumulation of MET occurred in PCa cells in a concomitant fashion. IF staining showed that, in addition to the membrane localization, MET is also detected in nucleus of PC3 cells as detected by 3 different MET antibodies (Figure 2, A and B). To examine whether nMET is derived from the full-length MET (mMET), we treated PC3 cells with L685,456 (at 10μM for 1.5 h), a specific inhibitor of γ-secretase that has an catalytic cleavage activity on mMET. Our results showed that nMET accumulation was significantly decreased upon γ-secretase inhibitor treatment as compared with the control (Figure 2B). These data indicate that nMET is indeed the truncate form of the full-length MET in PCa cells, in agreement with the previous report (17). Cellular fractionation analysis confirmed that the MET detected in nucleus displayed a reduced molecular weight as compared with the full-length MET in cytosolic of both PC3 cells (Figure 2C) and DU145 cells (Supplemental Figure 2, B and C). These data demonstrated that endogenous nMET is found in human PCa cells, implicating a potential role in oncogenic function in vitro.

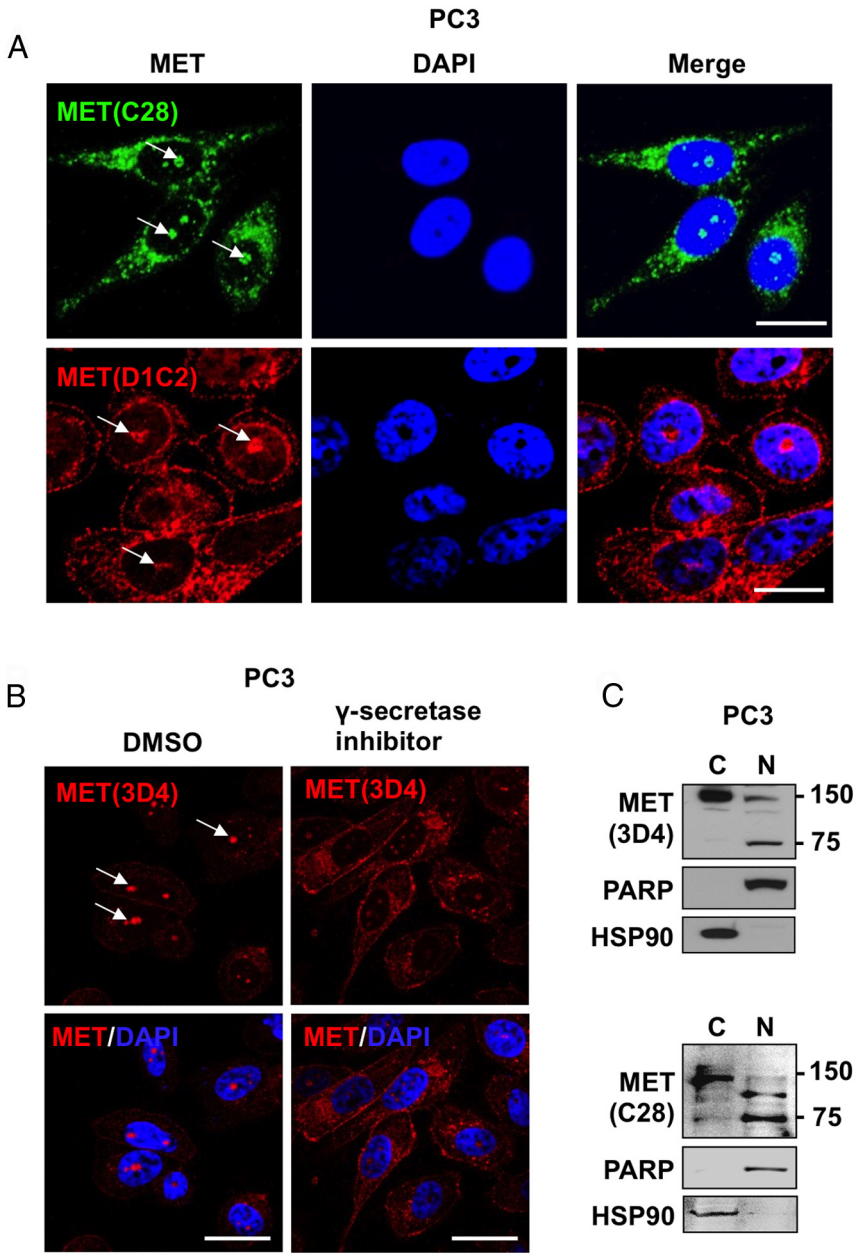

Figure 2. Endogenous expression of nuclear MET in human PCa cells. A, Endogenous MET protein in nuclei of PC3 cells using different MET antibodies. IF staining was performed with MET antibody (C28 or D1C2), and images were recorded with confocal microscopy. Representative images are shown from 3 independent experiments. Scale bars, 25 μm (top) and 15 μm (bottom). B, The decrease of nuclear MET expression in PC3 cells by γ-secretase inhibitor. PC3 cells were treated with γ-secretase inhibitor L685,456 (Abcam) at 10μM for 1.5 hours. IF was performed with MET antibody (3D4). Representative images are shown from 3 independent experiments. Scale bars, 25 μm. C, Cytoplasmic (C) and nuclear (N) fractionations of MET proteins in PC3 cells. PARP and HSP90 were used as markers for nuclear and cytosolic extracts of proteins, respectively. DAPI, 4′ 6-diamidino-2-phenylindole; DMSO, dimethyl sulfoxide.

Because *MET* gene transcription is repressed by AR (12), we reasoned that the level and the accumulation of MET in nucleus would be elevated upon androgen deprivation, a common approach of inhibiting AR. To this end, we chose to use LAPC4, an androgen-responsive PCa cell line expressing AR but a low level of MET. As demonstrated by IB and IF, levels of both endogenous nMET and SOX9 in LAPC4 cells were indeed increased upon androgen deprivation by culturing cells with medium containing charcoal-stripped FBS (cFBS) as compared with normal FBS (Figure 3, A–C). To further understand the biological relevance of the up-regulation of endogenous nMET and SOX9 in cells, we compared the growth of LAPC4-c cells (continuously cultured in cFBS, with elevated nMET and SOX9) with that of parental LAPC4 cells. As expected, parental LAPC4 cells proliferated slowly in cFBS culture condi-

tion. Surprisingly, LAPC4-c cells showed a significant increase of proliferation as compared with parental LAPC4 cells (Figure 3D). Moreover, spheroids formed in LAPC4-c cells were significantly increased under matrigel culture condition, companying with the induction of NANOG and OCT4 reprogramming factors (Figure 3E and Supplemental Figure 3A), whereas LAPC4 cells without spheres cells were negative for NANOG and OCT4. Consequently, the individual cells of spheres from LAPC4-c cells showed an increase in self-renewal ability as compared with that of parental cells (Figure 3F and Supplemental Figure 3, B and C). Consistent with the results above, LAPC4-c cells formed more primary spheres than that of parental LAPC4 cells under nonmatrigel sphere culture condition (Figure 3G). By contrast, MET knockdown by short hairpin RNA significantly reduced the spheres in LAPC4-c cells as compared with the control (Figure 3, H and I, and Supplemental Figure 3D). These data demonstrate that coup-regulation of endogenous nMET and SOX9 upon androgen deprivation may activate cell reprogramming to promote transformation and androgen-nonresponsive growth.

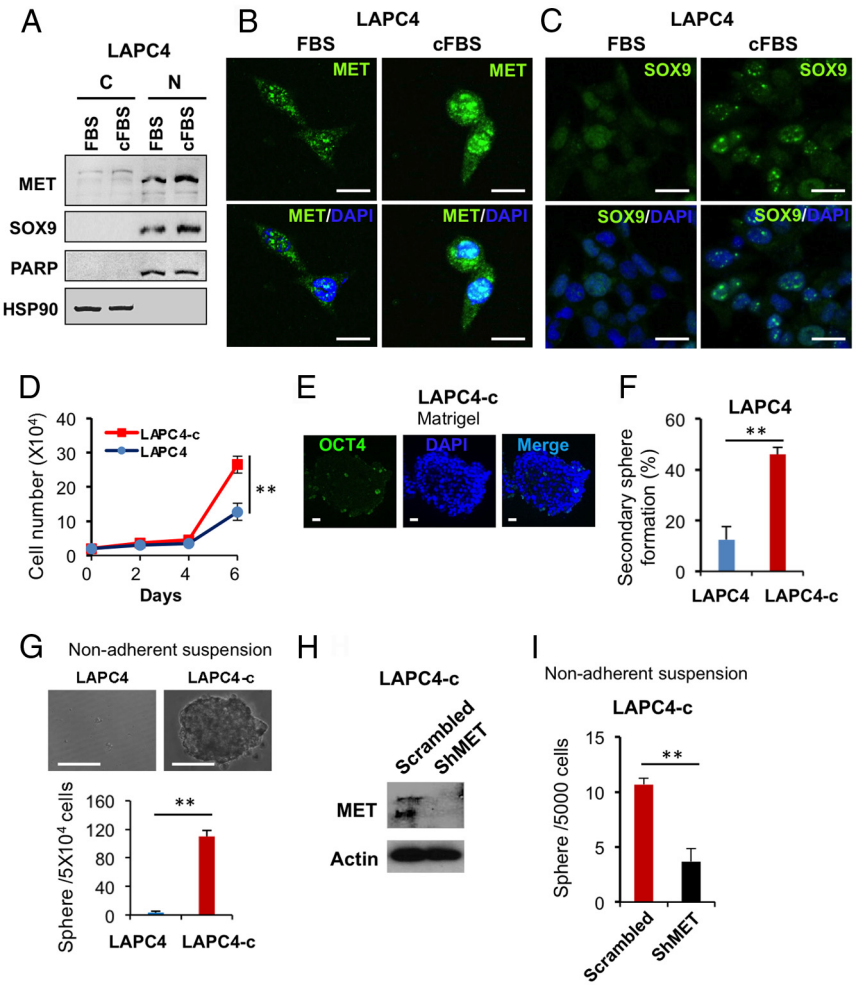

Figure 3. Androgen deprivation up-regulates endogenous nuclear MET and promotes stem-like cells self-renewal in androgen-responsive cells. A–C, Coup-regulation of endogenous nuclear MET and SOX9 in LAPC4 cells upon androgen depletion. LAPC4 cells were androgen depleted in cFBS medium for 10 days, and IB was performed using cytoplasmic and nuclear protein extracts (A). Representative images of IF probed with indicated antibodies (B and C). Scale bars, 25 μm. D, A comparison of growth curves between LAPC4-c and parental LAPC4 cells in androgen deprivation medium. E, IF staining on OCT4 reprogramming marker in spheroids of LAPC4-c cells in matrigel basement growth in medium with 2.5% cFBS. F, The self-renewal ability of LAPC4-c cells. Single spheroid forming cells were cultured in 96-well plates with nonmatrigel basement sphere culture medium described in Materials and Methods. G, Sphere formation of LAPC4-c cells in nonmatrigel basement sphere culture medium. Single cells were cultured in 96-well plates with sphere culture medium. Scale bars, 100 μm. H, The reduction of MET protein expression upon shMET knockdown in Western blotting. I, Suppression of the primary sphere formation in LAPC4-c cells upon MET knockdown. Single cells were cultured at a density of 500 cells/well in 96-well plates with sphere culture medium as described in Materials and Methods, and spheres were counted at 14 days. Error bars indicate SD.

Nuclear MET up-regulates SOX9 and activates β-catenin in PCa cells

Despite the full-length MET does not contain the nuclear localization sequence, yet MET can translocate into nonmembrane compartments of cells, including nucleus by cleavage (15). To further elucidate the oncogenic functions of nMET in PCa cells, we used the nMET construct in which the N-terminal transmembrane domain is deleted but the C-terminal cytoplasmic domain and kinase domain of MET are fused with GFP (15). We then wished to investigate downstream signaling pathways activated by nMET upon androgen deprivation. To this end, we chose to use 22Rv1 cells, in which the level of endogenous MET is low (Supplemental Figure 2A), to determine the changes of SOX9, an important factor in PCa. Our results showed that nMET overexpression resulted in a noticeable elevation of SOX9, and nMET was colocalized with SOX9 in nucleus of 22Rv1 cells (Supplemental Figure 4, A and B). In contrast, mMET overexpression or vector alone (expressing GFP tag) did not result in the induction of SOX9 in cells. To investigate the mechanism on SOX9 elevation induced by nMET, we overexpressed nMET in 293FT cells that express the endogenous SOX9 to understand the effect on the protein deg-

radation, whereas mMET and empty vector were used as the control. The immunoprecipitation and IB results showed that nMET overexpression resulted in a remarkable decrease of SOX9 polyubiquitination as compared with mMET and the empty vector (Supplemental Figure 4C). These results indicated that nMET elevation may contribute to the accumulation of SOX9 protein through preventing the ubiquitin-mediated proteasomal degradation. Together, these lines of evidence suggest a novel mechanism on SOX9 up-regulation by MET for cell functions in general.

Given the critical role of β-catenin in SOX9 expression and function (22), we then examined the effect of nMET on β-catenin in PCa cells. However, nMET overexpression in 293FT cells did not result in a significant increase of β-catenin level when whole-cell lysates were analyzed (data not shown). Because the active form of β-catenin is mainly localized in nucleus of cancer cells, we then performed cellular fractionations to examine the β-catenin level in the nuclear compartment of LAPC4 cells under androgen deprivation. Our results showed that the level of nuclear β-catenin was elevated upon mMET overexpression in the normal FBS condition as compared with nMET and the empty vector. Surprisingly, in androgen deprivation condition, nMET overexpression induced a noticeable increase of nuclear β-catenin than mMET (Figure 4A). In line with this finding, nMET overexpression in LAPC4 cells also remarkably increased the protein level of AR, a downstream target of β-catenin, as compared with mMET overexpression (Figure 4B). Consistent with the up-regulation of AR, nMET overexpression resulted in a significant increase of AR-mediated transcription of target genes determined by ARR2-PB-Luc reporter assay in an androgen deprivation condition (Figure 4C). Collectively, these results suggest that nMET may contribute to CRPC growth by activating SOX9 and β-catenin/AR signaling axis.

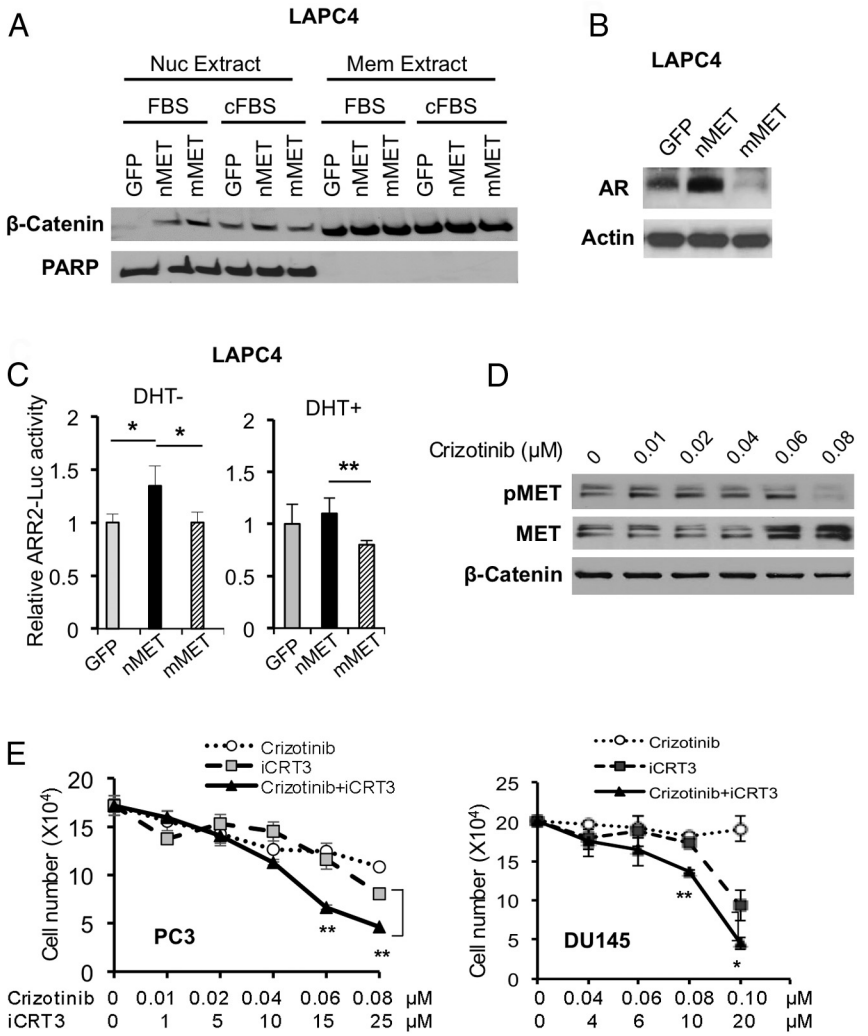

Figure 4. Nuclear MET activates β-catenin pathway and a combined inhibition of MET and β-catenin increases the efficiency. A, The level of nuclear β-catenin was increased by nMET overexpression in LAPC4 cells. B, The level of AR was increased by nMET overexpression in LAPC4 cells. C, ARR2-PB-Luc reporter assay showed that nMET contributes to AR activity. *, $P < .05$; **, $P < .01$ in Student's *t* test. D, MET inhibitor crizotinib decreased MET activity measured by autophosphorylation (pMET) at Tyr1234/1235 and slightly decreased β-catenin in PC3 cells. E, Combined inhibition of MET and β-catenin by crizotinib and iCRT3 suppressed the growth of PC3 and DU145 PCa cells. *, $P < .05$; **, $P < .01$ in Student's *t* test.

A combined inhibition of MET and β-catenin signaling efficiently suppresses the growth of hormone refractory PCa cells

The results above encouraged us to evaluate whether targeting both mMET and nMET/SOX9/β-catenin pathways would improve the efficacy of inhibiting the growth of PCa cells. Single treatment with either MET inhibitor, crizotinib (13), or β-catenin inhibitor, iCRT3, was reported to inhibit the growth of prostate or colon cancer cells (32). Our results showed that crizotinib treatment in PC3 cells resulted in a striking reduction of phospho-MET activity measured by autophosphorylation at Y1234/Y1235, whereas total β-catenin level decreased marginally (Figure 4D). To investigate the synergistic inhibitory effects of MET and nMET/SOX9/β-catenin pathways on the growth of castra-

tion-resistant cells, we performed a series of combinations of 2 inhibitors for treatment of PCa cells. Markedly, a combination treatment with crizotinib and iCRT3 resulted in a significant reduction of cell growth in PC3 and DU145 PCa cells (Figure 4E), both of which are androgen nonresponsive, with high levels MET/nMET and SOX9/β-catenin. The effective regimens were achieved with 60nM crizotinib and 15μM iCRT3 for PC3 cells and 80nM crizotinib and 10μM iCRT3 for DU145 cells. Our results indicated that crizotinib in combination with iCRT3 efficiently inhibited the growth of androgen-nonresponsive PCa cells.

Nuclear MET induces cell reprogramming in hormone refractory PCa cells

Due to the crucial role of cell reprogramming in the development and the progression of recurrent cancers, we assessed whether nMET overexpression contributes to the reprogramming process of PCa cells. We sought to choose C4–2B cell line because of its low level of MET expression and features in hormone refractory. Given that nMET is constitutively activated in cancer cells independent of HGF stimulus, we performed our experiments without addition of HGF. Consistent with these results above, expression of nMET, but not mMET or vector, led to elevations of SOX9 and nuclear β-catenin in C4–2B cells (Figure 5, A and B, and Supplemental Figure 5, A and B). We then wished to understand the biological implication of nMET overexpression in essential traits of stem cells. Because C4–2B cells have the high ability of forming spheroids in nonadherent sphere culture condition (33), we cultured C4–2B cells expressing nMET in the adherent matrigel condition to minimize the background. Importantly, an increased expression of NANOG was found in spheroids of C4–2B cells induced by nMET but barely detected in spheroids induced by mMET or the vector control (Figure 5C and Supplemental Figure 5C). In agreement with this notion, nMET overexpression significantly promoted spheroid formation of C4–2B cells in cFBS condition (Figure 5D). Similarly, overexpression of nMET, not mMET, increased the self-renewal ability of sphere forming cells in 22Rv1 cells (Figure 5E). Our results were in agreement with previous reports that 22Rv1 cells have low abilities in sphere formation and self-renewal (33). Our data suggest that nMET promotes 3-dimensional growth and transformation through inducing cell reprogramming in hormone refractory PCa cells.

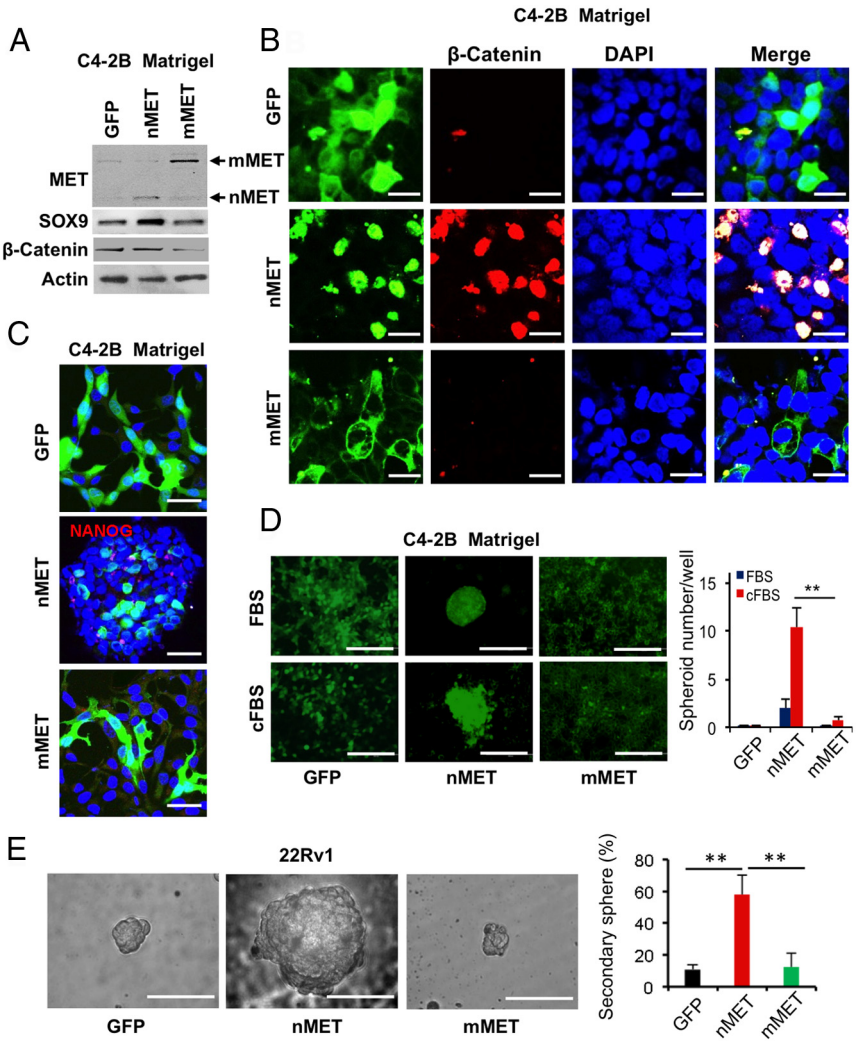

Figure 5. Nuclear MET overexpression promotes spheroid formation and self-renewal capacity. A, IB shows that nMET overexpression induces SOX9 levels in C4–2B cells. B, IF images show that nMET overexpression induces β-catenin in nuclei of C4–2B cells. Scale bars, 25 μm. The data are representatives of 3 independent experiments. C, nMET induces NANOG protein in nuclei of spheroids in C4–2B cells. Scale bars, 50 μm. D, nMET induces spheroids on matrigel in C4–2B cells. The spheroids were seeded into matrigel-treated plates and counted in triplicate. **, $P < .01$. Scale bars, 200 μm. The data are representatives of 3 independent experiments. E, nMET increases the self-renewal of spheroid forming cells. Prostate spheroids from matrigel basement growth were dissociated and diluted to single cells and then plated in 96-well plates for sphere forming assay in the sphere culture condition. Scale bars, 100 μm. **, $P < .01$. Error bars indicate SD. DAPI, 4′ 6-diamidino-2-phenylindole.

Elevations of nuclear Met in recurrent tumors in *Pten/Trp53* mutant mice in vivo

Literature reported that *Pten/Trp53* prostate-specific knockout

mice develop aggressive PCa and display the recurrent growth of CRPC (29, 30). Therefore, we decided to take advantage of this unique mouse model to validate the contributions of nuclear Met in prostate tumors and CRPC growth in vivo. We performed the surgical castration on *Pten/Trp53* mice at 3 months of age and then harvested recurrent prostate tumors from mutant mice 3 months after castration (Figure 6A). All castrated *Pten/Trp53* mice died of recurrent growth of PCa at 5–6 months of age (data not shown), so we examined whether Met was associated to the recurrent growth of PCa. Consistent with previous reports, prostate tumors of *Pten/Trp53* mice were full of poorly differentiated cancer cells (Figure 6B). Interestingly, IHC analysis revealed that Met accumulation in membrane was predominantly detected in malignant cells in naïve tumors but rarely found in recurrent tumors of castrated mutant mice (Figure 6C and Supplemental Figure 6). Surprisingly, Met accumulation in nucleus was predominantly detected in malignant cells in recurrent tumors of *Pten/Trp53* mice but rarely found in naïve tumors of age-matched control mice (Figure 6C). To confirm our findings on nMet, Sox9, and β-catenin in vivo in mice, we investigated whether Sox9 and β-catenin proteins were also up-regulated together with nMet in CRPC tumors of *Pten/Trp53* mice. As shown, Sox9 (Figure 6D) and β-catenin (Figure 6E) were strikingly elevated in nucleus of recurrent tumors as compared with naïve tumors of *Pten/Trp53* mice. Quantification analysis revealed the elevations of nMet, Sox9, and nuclear β-catenin in recurrent tumors (Figure 6, F and G), and these elevations were positively correlated with Ki67 expression, a proliferation marker of cancer cells (Supplemental Figure 6). Our in vivo data further supported that nMet plays a decisive role in CRPC growth by interacting with Sox9 and β-catenin pathways.

In summary, we have demonstrated that MET is found in nucleus of malignant cells in human CRPC samples, PCa cell lines, and CRPC tumors in mice. nMET activates SOX9, β-catenin/AR pathway to promote androgen-nonresponsive cell growth, and NANOG-mediated self-renewal of stem-like cells. Our findings revealed a novel nMET signaling pathway driving CRPC growth through cell reprogramming (Figure 6H).

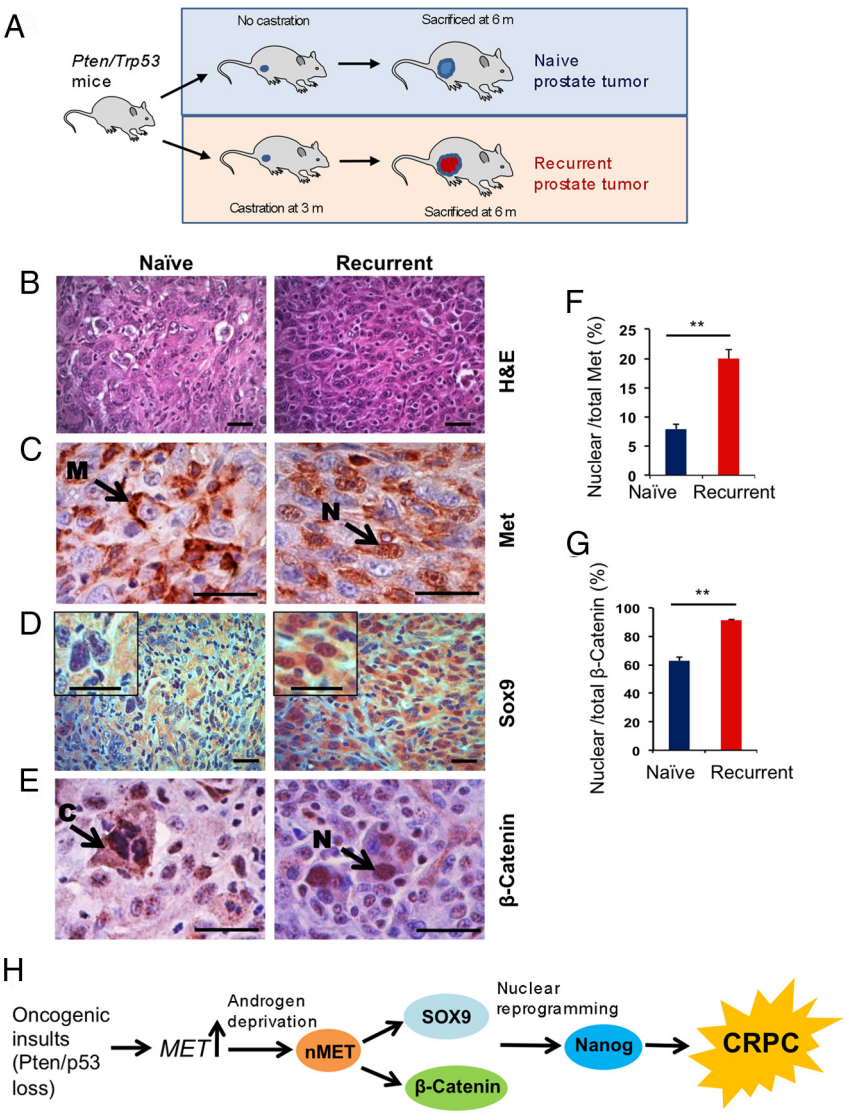

Figure 6. Up-regulation of nuclear MET in castration-resistant tumors of mice. A, A schematic outline to generate CRPC tumors in *Pten/Trp53* mutant mice. B, H&E staining and representative images of IHC staining of Met (C), Sox9 (D), and β-catenin (E) in naïve and recurrent prostate tumors of *Pten/Trp53* double null mice. Arrows indicate the staining in nucleus (N), membrane (M), or cytosol (C). Scale bars, 40 μm. F and G, Quantifications of IHC staining showed the percentage of cells with positive staining. **, $P < .01$. All data are shown as the mean ± SD. H, A working model on the network of nMET, SOX9, and β-catenin in CRPC progression.

Discussion

In this study, we reported for the first time both in vitro and in vivo a novel mechanism that MET contributes to CRPC through the dislocation in nucleus. RTKs implement essential biological functions, such as transcriptional regulation (34), DNA replication (35), DNA repair

(36), and drug resistance (37), through their locations in nuclei of cancer cells. Although full-length RTKs may shuttle between membrane and nuclear compartments (38), yet truncated forms of epidermal growth factor receptor (EGFR) (39) and erythroblastic leukemia viral oncogene homolog 4 (40) are found in nuclei of cancer cells. The full-length MET translocated into nucleus plays an important role in activating calcium signals (16). Interestingly, the truncated MET containing the cytoplasmic domain (or the C-terminal kinase domain) is termed as the nMET, which is fundamentally localized in nuclei of malignant cells (15), suggesting its connection with cancers. However, the oncogenic relevance and impact of nMET in PCa is unknown. In this study, we showed that the nMET overexpression is predominately localized in nucleus of PCa cells, such as C4–2B and LAPC4 cells, but with some distributions in cytoplasm of 22Rv1 cells (Supplemental Figure 4A). These lines of evidence indicate that distinct signaling pathways in 22Rv1 cells may modulate the cellular localization or stability of nMET in a cellular environment-dependent manner, because AR variants are highly expressed. Moreover, we found that nMET overexpression in LAPC4 cells increased AR levels but with a minimum transcriptional activity under androgen deprivation. Further investigation is needed to understand how the feedback loop of AR/mMET and nMET/AR is regulated, because AR level and activity are 2 distinct cascade events in CRPC (41). Understanding this nMET pathway will provide valuable insights into the development of efficient treatment of CRPC.

It is intriguing that NANOG, a reprogramming factor, is up-regulated upon nMET but not mMET overexpression under normal physiological conditions without HGF stimulation. NANOG overexpression has been shown to promote cell growth of CRPC both in vitro and in vivo (42), but the mechanism on the activation of reprogramming factors by androgen depletion is elusive. Our findings revealed the HGF-independent induction of NANOG but not other reprogramming factors by nMET (data not shown), indicating the specific role of nMET in the tissue-specific reprogramming to drive CRPC growth from PCa. HGF is required for MET-induced cell reprogramming in glioblastoma (43) and PCa stem-like phenotypes (44). However, there is no report on how MET contributes to the cell reprogramming leading to the androgen-nonresponsive growth of PCa. Our results support that MET is essential for sphere formation in PCa cells, and MET knockdown by short hairpin RNA significantly decreased the sizes and numbers of spheroids. Given the potential role of cancer stem cells in CRPC (45), our data further suggest that nMET may impact CRPC growth through stem-like cells self-renewal induced by androgen deprivation.

Drug resistance still remains a big challenge to successfully treat advanced PCa, particularly for CRPC. Elevations of RTKs contribute to the drug resistance through activation of multiple downstream pathways, such as PI3K (46), MAPK (47), breast cancer resistance protein (48), and Pim-1 proto-oncogene/tumor suppressor gene p53 (49). Single treatment with 1 RTK inhibitor frequently failed to drug resistance caused by activation of other signaling pathways. For example, *MET* amplification is likely associated to the resistance of lung cancer cells to EGFR inhibitors (47), and HGF-mediated reactivation of MAPK and PI3K-AKT through MET contributes to the resistance to RAF inhibitor (14). Moreover, a combined application of RAF and MET inhibitors significantly inhibited cell proliferation than single application (14), indicating that a synergistic suppression of 2 signaling pathways may improve the efficacy on restraining tumor growth. We discovered a novel mechanism that nMET activated both SOX9 and β-catenin to drive CRPC growth. We revealed that the SOX9 elevation by nMET may be caused by the decreased ubiquitination in PCa cells, yet the detailed mechanisms on the contributions of posttranslational modifications in PCa deserve the further investigation (29). In addition, nMET-mediated regulation on β-catenin seems more challenging due to the complexity of canonical Wnt signaling pathways in cancers. We demonstrated that a combined inhibition of nMET/β-catenin and mMET efficiently suppressed the growth of hormone refractory PCa cells, and moreover, nMET is significantly elevated in CRPC specimens than naive PCa specimens. This notion suggests that targeting nMET would be a novel avenue for treatment of CRPC. Moreover, we found that nuclear EGFR was also up-regulated upon androgen depletion (data not shown). These data suggest that nuclear homeostasis of RTKs maybe act as a general oncogenic mechanism for proliferations of castration-resistant cells. Collectively, we elucidated that the subcellular dislocation of RTKs to nucleus under androgen ablation contributes to cell reprogramming in CRPC. Targeting these aberrantly subcellular-localized RTKs would provide a novel avenue for treatment of advanced and recurrent cancers.

Acknowledgments

We thank Dr C.L. Sawyers, Dr S.W. Hayward, Dr R. Jin, and Dr L. Stewart for providing cell lines; D. Rimm Lab for providing MET plasmids through Addgene; P.G. Addai for counting cells;

and Dr X. Yu for advice on Sox9 IHC. We also thank Dr Matusik for his critical reading of the manuscript.

Address all correspondence and requests for reprints to: Dr Zhenbang Chen, Department of Biochemistry and Cancer Biology, Meharry Medical College, 1005 Dr DB Todd Jr Boulevard, Nashville, TN 37208. E-mail: zchen@mmc.edu.

This work was supported in part by National Institutes of Health Grants MD004038 (to Z.C.), MD007586, CA163069 (to Meharry Medical College), and RR024975–01 and TR000445–06 (to Vanderbilt). Microscopy experiments and data analysis performed in this study were supported in part by NIH Grants MD007593 and RR0254970.

Disclosure Summary: The authors have nothing to disclose.

References

1. **Huggins C, Hodges CV.** Studies on prostatic cancer. I. The effect of castration, of estrogen and androgen injection on serum phosphatases in metastatic carcinoma of the prostate. *CA Cancer J Clin*. 1972;22(4):232–240.
2. **Petrylak DP, Tangen CM, Hussain MH, et al.** Docetaxel and estramustine compared with mitoxantrone and prednisone for advanced refractory prostate cancer. *N Engl J Med*. 2004;351(15):1513–1520.
3. **Domingo-Domenech J, Vidal SJ, Rodriguez-Bravo V, et al.** Suppression of acquired docetaxel resistance in prostate cancer through depletion of notch- and hedgehog-dependent tumor-initiating cells. *Cancer Cell*. 2012;22(3):373–388.
4. **Linn DE, Yang X, Sun F, et al.** A role for OCT4 in tumor initiation of drug-resistant prostate cancer cells. *Genes Cancer*. 2010;1(9):908–916.
5. **Mulholland DJ, Kobayashi N, Ruscetti M, et al.** Pten loss and RAS/MAPK activation cooperate to promote EMT and metastasis initiated from prostate cancer stem/progenitor cells. *Cancer Res*. 2012;72(7):1878–1889.
6. **Carver BS, Chapinski C, Wongvipat J, et al.** Reciprocal feedback regulation of PI3K and androgen receptor signaling in PTEN-deficient prostate cancer. *Cancer Cell*. 2011;19(5):575–586.
7. **Linn DE, Yang X, Xie Y, et al.** Differential regulation of androgen receptor by PIM-1 kinases via phosphorylation-dependent recruitment of distinct ubiquitin E3 ligases. *J Biol Chem*. 2012;287(27):22959–22968.
8. **Guo Z, Dai B, Jiang T, et al.** Regulation of androgen receptor activity by tyrosine phosphorylation. *Cancer Cell*. 2006;10(4):309–319.
9. **Lu W, Xie Y, Ma Y, Matusik RJ, Chen Z.** ARF represses androgen receptor transactivation in prostate cancer. *Mol Endocrinol*. 2013;27(4):635–648.
10. **Cai C, He HH, Chen S, et al.** Androgen receptor gene expression in prostate cancer is directly suppressed by the androgen receptor through recruitment of lysine-specific demethylase 1. *Cancer Cell*. 2011;20(4):457–471.
11. **Gherardi E, Birchmeier W, Birchmeier C, Vande Woude G.** Targeting MET in cancer: rationale and progress. *Nat Rev Cancer*. 2012;12(2):89–103.
12. **Verras M, Lee J, Xue H, Li TH, Wang Y, Sun Z.** The androgen receptor negatively regulates the expression of c-Met: implications for a novel mechanism of prostate cancer progression. *Cancer Res*. 2007;67(3):967–975.
13. **Yoshioka T, Otero J, Chen Y, et al.** β4 Integrin signaling induces expansion of prostate tumor progenitors. *J Clin Invest*. 2013;123(2):682–699.
14. **Straussman R, Morikawa T, Shee K, et al.** Tumour micro-environment elicits innate resistance to RAF inhibitors through HGF secretion. *Nature*. 2012;487(7408):500–504.
15. **Pozner-Moulis S, Pappas DJ, Rimm DL.** Met, the hepatocyte growth factor receptor, localizes to the nucleus in cells at low density. *Cancer Res*. 2006;66(16):7976–7982.
16. **Gomes DA, Rodrigues MA, Leite MF, et al.** c-Met must translocate to the nucleus to initiate calcium signals. *J Biol Chem*. 2008;283(7):4344–4351.
17. **Nath D, Williamson NJ, Jarvis R, Murphy G.** Shedding of c-Met is regulated by crosstalk between a G-protein coupled receptor and the EGF receptor and is mediated by a TIMP-3 sensitive metalloproteinase. *J Cell Sci*. 2001;114(pt 6):1213–1220.
18. **Athauda G, Giubellino A, Coleman JA, et al.** c-Met ectodomain shedding rate correlates with malignant potential. *Clin Cancer Res*. 2006;12(14 pt 1):4154–4162.
19. **Guo W, Keckesova Z, Donaher JL, et al.** Slug and Sox9 cooperatively determine the mammary stem cell state. *Cell*. 2012;148(5):1015–1028.
20. **Seymour PA, Freude KK, Tran MN, et al.** SOX9 is required for maintenance of the pancreatic progenitor cell pool. *Proc Natl Acad Sci USA*. 2007;104(6):1865–1870.
21. **Cai C, Wang H, He HH, et al.** ERG induces androgen receptor-mediated regulation of SOX9 in prostate cancer. *J Clin Invest*. 2013;123(3):1109–1122.
22. **Wang H, McKnight NC, Zhang T, Lu ML, Balk SP, Yuan X.** SOX9 is expressed in normal prostate basal cells and regulates androgen receptor expression in prostate cancer cells. *Cancer Res*. 2007;67(2):528–536.
23. **Chesire DR, Isaacs WB.** β-Catenin signaling in prostate cancer: an early perspective. *Endocr Relat Cancer*. 2003;10(4):537–560.
24. **Sanges D, Romo N, Simonte G, et al.** Wnt/β-catenin signaling triggers neuron reprogramming and regeneration in the mouse retina. *Cell Rep*. 2013;4(2):271–286.
25. **Thomsen MK, Ambroisine L, Wynn S, et al.** SOX9 elevation in the prostate promotes proliferation and cooperates with PTEN loss to drive tumor formation. *Cancer Res*. 2010;70(3):979–987.
26. **Mulholland DJ, Tran LM, Li Y, et al.** Cell autonomous role of PTEN in regulating castration-resistant prostate cancer growth. *Cancer Cell*. 2011;19(6):792–804.
27. **Lunardi A, Ala U, Epping MT, et al.** A co-clinical approach identifies mechanisms and potential therapies for androgen deprivation resistance in prostate cancer. *Nat Genet*. 2013;45(7):747–755.
28. **Xie Y, Burcu M, Linn DE, Qiu Y, Baer MR.** Pim-1 kinase protects P-glycoprotein from degradation and enables its glycosylation and cell surface expression. *Mol Pharmacol*. 2010;78(2):310–318.
29. **Xie Y, Liu S, Lu W, et al.** Slug regulates E-cadherin repression via p19Arf in prostate tumorigenesis [published online May 21, 2014]. *Mol Oncol*. doi:10.1016/j.molonc.2014.05.006.
30. **Chen Z, Trotman LC, Shaffer D, et al.** Crucial role of p53-dependent cellular senescence in suppression of Pten-deficient tumorigenesis. *Nature*. 2005;436(7051):725–730.
31. **Choudhary C, Olsen JV, Brandts C, et al.** Mislocalized activation of oncogenic RTKs switches downstream signaling outcomes. *Mol Cell*. 2009;36(2):326–339.
32. **Gonsalves FC, Klein K, Carson BB, et al.** An RNAi-based chemical genetic screen identifies three small-molecule inhibitors of the Wnt/wingless signaling pathway. *Proc Natl Acad Sci USA*. 2011;108(15):5954–5963.
33. **Chen Z, Carracedo A, Lin HK, et al.** Differential p53-independent outcomes of p19(Arf) loss in oncogenesis. *Sci Signal*. 2009;2(84):ra44.
34. **Lin SY, Makino K, Xia W, et al.** Nuclear localization of EGF receptor and its potential new role as a transcription factor. *Nat Cell Biol*. 2001;3(9):802–808.
35. **Wang SC, Nakajima Y, Yu YL, et al.** Tyrosine phosphorylation controls PCNA function through protein stability. *Nat Cell Biol*. 2006;8(12):1359–1368.

36. **Fan S, Ma YX, Gao M, et al.** The multisubstrate adapter Gab1 regulates hepatocyte growth factor (scatter factor)-c-Met signaling for cell survival and DNA repair. *Mol Cell Biol*. 2001;21(15): 4968–4984.
37. **Li C, Iida M, Dunn EF, Ghia AJ, Wheeler DL.** Nuclear EGFR contributes to acquired resistance to cetuximab. *Oncogene*. 2009; 28(43):3801–3813.
38. **Wang YN, Hung MC.** Nuclear functions and subcellular trafficking mechanisms of the epidermal growth factor receptor family. *Cell Biosci*. 2012;2(1):13.
39. **Edwards J, Traynor P, Munro AF, Pirret CF, Dunne B, Bartlett JM.** The role of HER1-HER4 and EGFRvIII in hormone-refractory prostate cancer. *Clin Cancer Res*. 2006;12(1):123–130.
40. **Ni CY, Murphy MP, Golde TE, Carpenter G.** γ-Secretase cleavage and nuclear localization of ErbB-4 receptor tyrosine kinase. *Science*. 2001;294(5549):2179–2181.
41. **Qi J, Tripathi M, Mishra R, et al.** The E3 ubiquitin ligase Siah2 contributes to castration-resistant prostate cancer by regulation of androgen receptor transcriptional activity. *Cancer Cell*. 2013; 23(3):332–346.
42. **Jeter CR, Liu B, Liu X, et al.** NANOG promotes cancer stem cell characteristics and prostate cancer resistance to androgen deprivation. *Oncogene*. 2011;30(36):3833–3845.
43. **Li Y, Li A, Glas M, et al.** c-Met signaling induces a reprogramming network and supports the glioblastoma stem-like phenotype. *Proc Natl Acad Sci USA*. 2011;108(24):9951–9956.
44. **van Leenders GJ, Sookhlall R, Teubel WJ, et al.** Activation of c-MET induces a stem-like phenotype in human prostate cancer. *PLoS One*. 2011;6(11):e26753.
45. **Hynes PG, Kelly K.** Prostate cancer stem cells: the case for model systems. *J Carcinog*. 2012;11:6.
46. **Samuels Y, Wang Z, Bardelli A, et al.** High frequency of mutations of the PIK3CA gene in human cancers. *Science*. 2004;304(5670): 554.
47. **Solit DB, Garraway LA, Pratilas CA, et al.** BRAF mutation predicts sensitivity to MEK inhibition. *Nature*. 2006;439(7074):358–362.
48. **Huang WC, Chen YJ, Li LY, et al.** Nuclear translocation of epidermal growth factor receptor by Akt-dependent phosphorylation enhances breast cancer-resistant protein expression in gefitinib-resistant cells. *J Biol Chem*. 2011;286(23):20558–20568.
49. **Xie Y, Xu K, Dai B, et al.** The 44 kDa Pim-1 kinase directly interacts with tyrosine kinase Etk/BMX and protects human prostate cancer cells from apoptosis induced by chemotherapeutic drugs. *Oncogene*. 2006;25(1):70–78.